CHEMISTRY
A EUROPEAN JOURNAL

Water-Insoluble Ag–U–Organic Assemblies with Photocatalytic Activity

Zhen-Tao Yu, Zuo-Lei Liao, Yu-Sheng Jiang, Guang-Hua Li, and Jie-Sheng Chen*[a]

Abstract: Two metal–organic coordination polymers $[Ag(bipy)(UO_2)(bdc)_{1.5}]$ (bipy = 2,2′-bipyridyl, bdc = 1,4-benzenedicarboxylate) and $[Ag_2(phen)_2UO_2(btec)]$ (phen = 1,10-phenanthroline, btec = 1,2,4,5-benzenetetracarboxylate) were obtained by hydrothermal assembly of the d^{10} metal silver and the 5f metal uranium with mixed ligands. Both compounds form two-dimensional networks with π–π overlap interactions between the aromatic fragments in the neighboring layers. In aqueous suspension the two water-insoluble materials show photocatalytic degradation performance superior to that of commercial TiO_2 (Degussa P-25) when tested on nonbiodegradable rhodamine B (RhB) as model pollutant. The relationship between the structure of the photocatalysts and the photocatalytic activity was also elucidated. On the basis of the monitored intermediate species and the final mineralized products, it is proposed that the possible reaction mechanism for the photodegradation (oxidation) of RhB in aqueous solution catalyzed by the two assembly compounds involves photoexcitation of uranyl centers and molecular oxygen.

Keywords: heterogeneous catalysis · hydrothermal synthesis · photochemistry · silver · uranium

Introduction

The construction of metal–organic assemblies is currently attracting considerable attention in view of their interesting structural topologies and physicochemical properties.[1] A variety of metal–organic assemblies have been synthesized, and most of them involve the d-block transition metals.[2] Whereas 4f metals were also reported to form such assemblies,[3] the 5f metals have seldom been used as nodes for the assembly of organic-bridged coordination networks,[4] although the importance of uranium-containing materials with magnetic,[5] optical,[6] thermal catalytic,[7] ion-exchange,[8] and N_2-fixation properties[9] has been addressed in the literature.

Photocatalysis is being used for the green ecological elimination of organic dirt or harmful pollutants,[10] but it is also attracting increasing interest as a potentially clean and renewable source for hydrogen fuel by splitting of water into H_2 and O_2 by means of solar-to-chemical conversion.[11] Typical solid photocatalysts commonly used are semiconductor metal oxide and sulfide particles such as TiO_2, ZnO, WO_3, CdS, ZnS, and Fe_2O_3; layered niobates and titanates; and polyoxometallates (POM), mainly of W.[10,12] However, most wide-band-gap catalysts rely on UV light for excitation, and this limits their practical applications because of the expensive overall process.[13] Some narrow-band-gap semiconductors such as CdS and CdSe are photochemically unstable in water since they are sensitive to photocorrosion.[14] In this regard, it is necessary to modify the wide-band-gap semiconductor compounds with other substitutional anionic species such as nitrogen,[15] sulfur,[16] and carbon;[17] suitable cationic or ion-implanted metals such as Pt, Pd, Au, Ag, Cr, Mn, Fe, and Cu;[18] and other coupled or capped semiconductor oxides.[19] These modifiers act as charge separators of the photoinduced electron–hole pair and thus extend and improve the photoactivity and allow the use of the main visible-light range of the solar spectrum.[20]

On the other hand, it is also of interest to search for new photocatalytic solids with improved properties even when irradiated with cheaper visible light ($\lambda > 380$ nm) in the main part of the solar spectrum.[15] Recent studies have shown that aqueous solutions of uranyl ions are photocatalytically active for oxidation of organic substrates at long wavelengths in the presence of air.[21] However, difficult separation of the uranyl ions from the reaction system renders this catalyst system less practical. We have been interested in the synthesis and characterization of new uranium-contain-

[a] Dr. Z.-T. Yu, Z.-L. Liao, Y.-S. Jiang, G.-H. Li, Prof. Dr. J.-S. Chen
State Key Laboratory of Inorganic Synthesis and Preparative Chemistry
College of Chemistry, Jilin University
Changchun 130012 (P. R. China)
Fax: (+86) 431-516-8624
E-mail: chemcj@mail.jlu.edu.cn

Supporting information for this article is available on the WWW under http://www.chemeurj.org/ or from the author.

DOI: 10.1002/chem.200401189

ing materials which show rich structural features and encouraging photophysical properties.[6,22] In particular, the discovery of photocatalytic activity of a 3D U-containing solid compound[23] prompted us to synthesize water-insoluble organic–inorganic uranyl materials with improved photocatalytic performance. Here we describe two bimetallic 2D assemblies, $[Ag(bipy)(UO_2)_2(bdc)_{1.5}]$ (**1**; bipy = 2,2′-bipyridyl, bdc = 1,4-benzenedicarboxylate) and $[Ag_2(phen)_2UO_2(btec)]$ (**2**; phen = 1,10-phenanthroline; btec = 1,2,4,5-benzenetetracarboxylate), both of which are water-insoluble and more active than nanosized TiO_2 (P-25) for the degradation of rhodamine B, a cationic N-containing dye which is generally recognized as being difficult to degrade.

Results and Discussion

Synthesis and characterization: The nature of chelating bidentate nitrogen-donor ligands as building blocks with extended planar π systems (e.g., 1,10-phenanthroline and 2,2′-bipyridyl), which can be used in preparing model compounds to mimic noncovalent, supramolecular interactions in biological processes,[24] may potentially lead to supramolecular arrays with π–π aromatic stacking interactions that usually result in coordination polymers with lower dimensionality.[25] On the basis of these considerations and the interesting topologies and coordination chemistry of silver and uranyl cations, we prepared two 2D bimetallic compounds with unique architectures in a relatively straightforward fashion by means of conventional hydrothermal reactions. Compounds **1** and **2** were obtained as pure single-phase products, as confirmed by inductively coupled plasma (ICP) and elemental (C, H, N) analyses, and by comparison of the observed powder XRD patterns with those generated from single-crystal structural data.

The IR spectra of **1** and **2** in KBr show intense absorption bands between 800 and 950 cm^{-1}. The bands at about 920 and 850 cm^{-1} are most reasonably assigned to the asymmetric and symmetric O=U=O stretching modes of the uranyl moiety,[26] respectively. The IR spectra confirm that the uranium species in **1** and **2** is U^{VI}, because the frequencies of the observed bands are consistent with the asymmetric and symmetric stretching bands in most uranyl(VI) complexes. The bands at 1438 and 1482 cm^{-1} for **1** and **2** correspond to skeletal vibrations of the aromatic rings[26] with their out-of-plane vibrations at 750 and 767 cm^{-1} for **1** and **2**, respectively.

The thermal properties of **1** and **2** were determined by recording their thermogravimetric/differential thermal analysis (TG/DTA) curves in air. From the TG curve, the total weight loss of **1** of 49.9%, attributable to removal of the total organic component, is in agreement with the calculated value based on the single-crystal structure of **1** (51.5%). The total weight loss of **2** of 56.0%, again corresponding to the removal of the total organic component, is also in accordance with the calculated value (55.7%). The TG/DTA data indicate that both **1** and **2** are thermally stable up to approximately 300 °C, in agreement with the powder XRD patterns.

Crystal structures: Crystallographic data and structure refinement parameters for **1** and **2** are summarized in Table 1. Selected bond lengths and angles are given in Tables 2 and 3, respectively, and the metal–ligand coordination in **1** and **2** is detailed in Figures 1 and 2, respectively. In **1**, each uranium atom is located in a pentagonal-bipyramidal environ-

Table 1. Crystal data and structure refinement for **1** and **2**.

	1	**2**
empirical formula	$C_{22}H_{14}AgN_2O_8U$	$C_{34}H_{18}Ag_2N_4O_{10}U$
formula weight	780.25	1096.29
T [K]	293(2)	293(2)
crystal system	triclinic	monoclinic
space group	$P\bar{1}$	$C2/c$
a [Å]	9.1166(5)	22.6428(6)
b [Å]	10.0836(5)	7.3174(2)
c [Å]	12.1438(8)	18.4324(6)
α [°]	79.391(3)	90
β [°]	87.550(3)	107.011(2)
γ [°]	78.848(2)	90
V [Å^3]	1076.53(11)	2920.38(15)
Z	2	4
ρ [Mg m^{-3}]	2.407	2.493
μ [mm^{-1}]	8.476	6.934
$F(000)$	726	2064
θ range [°]	2.45–25.07	1.88–30.03
Limiting indices	$-9 \le h \le 10$	$-31 \le h \le 31$
	$-11 \le k \le 11$	$-10 \le k \le 9$
	$-14 \le l \le 13$	$-25 \le l \le 14$
reflections collected/unique	6014/3738	11388/4265
	[R(int) = 0.0512]	[R(int) = 0.0472]
data/parameters	3738/307	4265/231
$R1$[a]/$wR2$[b] [$I > 2\sigma(I)$]	0.0336/0.0864	0.0303/0.0650
$R1$/$wR2$ (all data)	0.0362/0.0893	0.0340/0.0660
largest diff. peak/hole [e Å^{-3}]	2.219/−1.797	1.532/−2.091

[a] $R1 = \Sigma ||F_o| - |F_c|| / \Sigma |F_o|$. [b] $wR2 = [\Sigma w(F_o^2 - F_c^2)^2 / \Sigma w(F_o^2)^2]^{1/2}$.

Table 2. Selected bond lengths [Å] and angles [°] for **1**.[a]

U(1)-O(7)	1.766(5)	U(1)-O(5)	2.346(5)
U(1)−O(8)	1.772(6)	U(1)−O(2)	2.418(5)
U(1)−O(3)	2.316(5)	U(1)−O(1)	2.507(5)
U(1)−O(4)#1	2.321(5)		
Ag(1)−O(6)	2.235(6)	Ag(1)−N(1)	2.345(9)
Ag(1)−N(2)	2.298(7)		
O(7)-U(1)-O(8)	179.4(3)	O(8)-U(1)-O(2)	91.6(2)
O(7)-U(1)-O(3)	88.3(3)	O(3)-U(1)-O(2)	126.45(17)
O(8)-U(1)-O(3)	91.1(2)	O(4)#1-U(1)-O(2)	148.67(17)
O(7)-U(1)-O(4)#1	90.4(3)	O(5)-U(1)-O(2)	70.92(16)
O(8)-U(1)-O(4)#1	89.4(3)	O(7)-U(1)-O(1)	94.1(2)
O(3)-U(1)-O(4)#1	84.82(17)	O(8)-U(1)-O(1)	85.8(2)
O(7)-U(1)-O(5)	90.4(2)	O(3)-U(1)-O(1)	74.52(16)
O(8)-U(1)-O(5)	90.1(2)	O(4)#1-U(1)-O(1)	158.68(18)
O(3)-U(1)-O(5)	162.53(17)	O(5)-U(1)-O(1)	122.95(16)
O(4)#1-U(1)-O(5)	77.77(17)	O(2)-U(1)-O(1)	52.40(16)
O(7)-U(1)-O(2)	88.9(3)		
O(6)-Ag(1)-N(2)	169.0(2)	N(2)-Ag(1)-N(1)	71.8(3)
O(6)-Ag(1)-N(1)	112.8(3)		

[a] Symmetry transformations used to generate equivalent atoms: #1: $-x+1, -y, -z+1$.

Table 3. Selected bond lengths [Å] and angles [°] for **2**.[a]

U(1)–O(5)	1.770(3)	U(1)–O(3)#2	2.526(3)
U(1)–O(5)#1	1.770(3)	U(1)–O(3)#3	2.526(3)
U(1)–O(1)#1	2.404(2)	U(1)–O(4)#2	2.564(3)
U(1)–O(1)	2.404(2)	U(1)–O(4)#3	2.564(3)
Ag(1)–O(1)	2.362(3)	Ag(1)–N(2)	2.365(4)
Ag(1)–O(2)#1	2.520(3)	Ag(1)–N(1)	2.374(4)
O(5)-U(1)-O(5)#1	179.29(17)	O(3)#2-U(1)-O(3)#3	62.48(13)
O(5)-U(1)-O(1)#1	93.67(11)	O(5)-U(1)-O(4)#2	96.90(12)
O(5)#1-U(1)-O(1)#1	85.76(11)	O(5)#1-U(1)-O(4)#2	83.24(12)
O(5)-U(1)-O(1)	85.76(11)	O(1)#1-U(1)-O(4)#2	136.00(8)
O(5)#1-U(1)-O(1)	93.67(11)	O(1)-U(1)-O(4)#2	65.99(8)
O(1)#1-U(1)-O(1)	72.41(12)	O(3)#2-U(1)-O(4)#2	50.77(8)
O(5)-U(1)-O(3)#2	81.87(12)	O(3)#3-U(1)-O(4)#2	107.54(9)
O(5)#1-U(1)-O(3)#2	98.75(12)	O(5)-U(1)-O(4)#3	83.24(12)
O(1)#1-U(1)-O(3)#2	172.67(9)	O(5)#1-U(1)-O(4)#3	96.90(12)
O(1)-U(1)-O(3)#2	112.83(9)	O(1)#1-U(1)-O(4)#3	65.99(8)
O(5)-U(1)-O(3)#3	98.75(12)	O(1)-U(1)-O(4)#3	136.00(8)
O(5)#1-U(1)-O(3)#3	81.87(12)	O(3)#2-U(1)-O(4)#3	107.54(9)
O(1)#1-U(1)-O(3)#3	112.83(9)	O(3)#3-U(1)-O(4)#3	50.77(8)
O(1)-U(1)-O(3)#3	172.67(9)	O(4)#2-U(1)-O(4)#3	157.67(12)
N(2)-Ag(1)-N(1)	71.6(6)	N(2)-Ag(1)-O(8)#3	81.1(5)
N(2)-Ag(1)-O(3)	140.4(5)	N(1)-Ag(1)-O(8)#3	141.9(6)
N(1)-Ag(1)-O(3)	126.5(5)	O(3)-Ag(1)-O(8)#3	91.4(4)
O(7)-Ag(2)-N(3)	121.2(5)	O(7)-Ag(2)-O(4)#4	89.9(4)
O(7)-Ag(2)-N(4)	140.8(5)	N(3)-Ag(2)-O(4)#4	148.9(6)
N(3)-Ag(2)-N(4)	69.5(6)	N(4)-Ag(2)-O(4)#4	85.6(5)

[a] Symmetry transformations used to generate equivalent atoms: #1: $-x$, y, $-z+1/2$; #2: x, $y-1$, z; #3: $-x$, $y-1$, $-z+1/2$; #4: x, $y+1$, z; #5: $-x$, $-y+2$, $-z$.

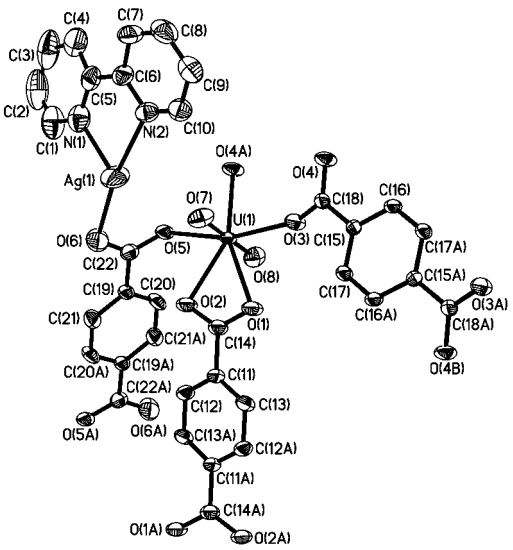

Figure 1. The building block including the asymmetric unit present in **1** with non-hydrogen atoms represented by thermal ellipsoids at 50% probability.

ment, surrounded by seven oxygen atoms, five of which are in the equatorial plane and are from three bdc ligands. The remaining two O atoms are terminal and occupy the two axial positions to complete the coordination sphere of the U^{VI} center. The bond lengths of the UO_7 moiety vary from 1.766(5) to 1.772(6) Å for the axial U=O bonds, and from 2.316(5) to 2.507(5) Å for the U–O bonds.[27] As shown in

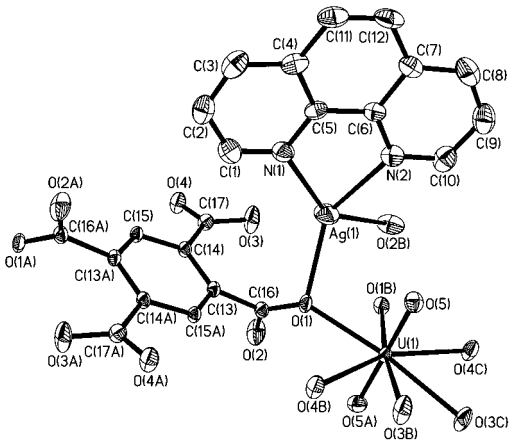

Figure 2. The building block including the asymmetric unit present in **2**. Thermal ellipsoids drawn at 50% probability; hydrogen atoms omitted for clarity.

Figure 3a, the structure of **1** comprises bridging bdc ligands, $[Ag(bipy)]^+$ units, and uranyl ions, which form a neutral 2D layer in the *ac* plane. The carboxylate groups of one bdc bridge two uranium centers in a bis-bidentate fashion, and the additional two bdc ligands each bind two uranyl ions and two $[Ag(bipy)]^+$ units through the four CO groups. The Ag atom is coordinated in a distorted T-shaped geometry by two N atoms from the bipy ligand (Ag–N 2.298(7), 2.345(9) Å) and one O atom from the bdc ligand (Ag–O 2.235(6) Å).[28] The uranyl units in **1** are connected by bridging bdc ligands to form chains, which are then cross-linked by

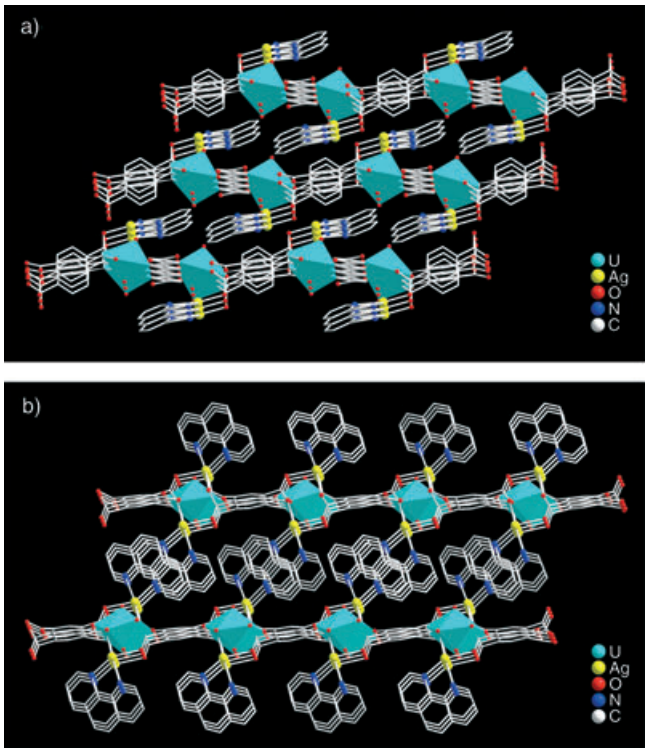

Figure 3. View of the layer packing for a) **1** and b) **2** along the *b* axis.

additional bdc groups to generate a 2D network decorated with $[Ag(bipy)]^+$ subunits that project into the interlamellar regions above and below the layer. The 2D layers stack along the *b* axis through edge-to-face π–π interactions[29] between bdc and bipy ligands in neighboring layers.

The coordination sphere at the uranium site of **2** is defined by two axial oxygen donors (U–O 1.770(3) Å) and an equatorial plane occupied by six oxygen donors from two chelating and two monodentate carboxyl groups of btec ligands (U–O 2.404(2)–2.564(3) Å; Figure 2). The four-coordinate Ag^I center has a coordination environment inbetween tetrahedral and square-planar, with two oxygen atoms from the monodentate carboxyl groups of btec ligands (Ag–O 2.362(3), 2.520(3) Å) and two nitrogen donors from chelating phen groups (Ag–N 2.365(4), 2.374(4) Å).[28] The extended structure of **2** consists of a 2D layered network with Ag-UO_8-Ag trinuclear cores as building units, which are linked by the bridging btec ligands (Figure 3b). The pairs of phen ligands from adjacent layers are arranged in an interdigitating manner leading to offset face-to-face π–π stacking[29] along the *b* axis, which seems to be the driving force for the stabilization of solid **2**.

Photocatalytic properties: The diffuse-reflectance UV/Vis spectra reveal that solid **1** and **2** have similar absorption features (Figure 4). Both spectra consist of absorption components in the UV and Vis regions. The UV component is attributed to charge-transfer electronic transition of the uranyl group, that is, from the doubly bonded O 2p bonding orbital to the nonbonding or antibonding orbitals of the uranium ion,[30] and the Vis component responsible for the color of the compounds may arise from ligand-to-metal charge transfer (LMCT) between the O atoms of the coordinating ligand and an empty orbital on the U^{VI} ions.[31] In spite of certain similarities in UV/Vis absorption behavior for **1** and **2**, it could be noted by careful comparison of the two absorption curves (in Kubelka–Munk units) that the onset of the charge-transfer transition of **1** occurs in the visible region, while that of **2** lies in the near-UV region, and the absorption of **2** in the visible region is not as distinct as that of **1**. The presence of charge-transfer transitions motivated us to explore applications of **1** and **2** in heterogeneous photocatalysis.

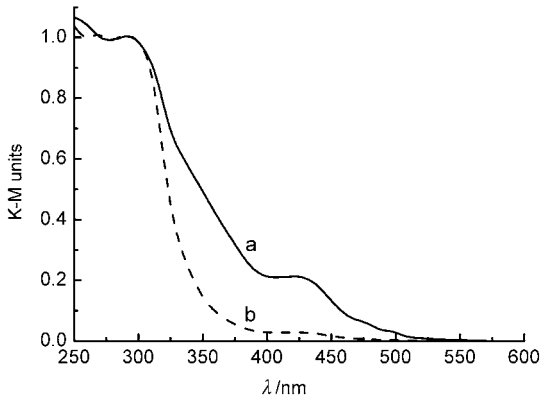

Figure 4. UV/Vis diffuse-reflectance spectra of as-synthesized **1** (a) and **2** (b) with $BaSO_4$ as background.

The photodegradation activity was tested by using a solution of nonbiodegradable rhodamine B (RhB) as a target pollutant for degradation experiments.[32] For comparison, the photocatalytic performance of commercial TiO_2 (Degussa P-25) was also assessed under the same experimental conditions. Control experiments were conducted on an RhB solution in the absence of particles of **1** or **2**. Only a very small decrease in intensity for the characteristic UV/Vis absorption of RhB was observed for UV irradiation times shorter than 60 min, and complete disappearance of RhB in aqueous solution required about 600 min in the absence of photocatalysts. When an RhB suspension containing powder catalyst **1** or **2** was stirred in the dark for at least 30 min under otherwise identical conditions, no intensity decrease was seen in the UV/Vis absorption spectrum in comparison with that of the original RhB solution.

The well-defined absorption peaks in the visible region corresponding to the parent dye disappear rapidly with a concomitant hypsochromic shift attributed to *N*-deethylation of RhB after photocatalysis in the presence of **1** or **2** (see Supporting Information),[33] which suggests that at least the chromophore responsible for the characteristic color of RhB is broken down and the degradation of dye proceeds in the presence of **1** or **2** particles. The distinctly shortened degradation time compared with the control experiments indicates that the catalyst **1** or **2** plays an important role in the photodecomposition of RhB. To rule out the possibility that under the experimental conditions the solid catalysts **1** and **2** are dissolved in the solutions and the catalytic activities result from soluble species instead of the original solids, we subjected the catalysts to UV irradiation and continuous stirring in water for 1 h for **1** and 2 h for **2** and tested the photocatalytic activity of the solution after filtering off the solid materials. No catalytic activity was observed for the thus-obtained solutions. Clearly the photocatalytic activities arise solely from the solids **1** and **2**.

Figure 5 shows the rate of RhB degradation (measured as RhB concentration versus irradiation time) in an aqueous solution in the presence of **1** and **2**. Both **1** and **2** are capable of photocatalyzing the degradation of the stable organic dye RhB upon application of a UV irradiation source (Hg lamp) and they display photocatalytic activities higher than that of P-25 ($[RhB] = 0.10\ mmol\,L^{-1}$, 80 mL dispersion, and loading of **1**, **2**, or P-25 of 160 mg, which in terms of metal content amounts to 0.20 or 0.15 mmol U and 2 mmol Ti, respectively). Since our compounds are powdered from large single crystals before tests, they should have less surface area and hence less accessible active centers than the same amount of the nanosized TiO_2 (ca. 30 nm). Hence, we concluded that our U^{VI} compounds are distinctly more efficient than P-25 in photocatalysis. After photocatalysis, both **1** and **2** show a powder XRD pattern nearly identical to that of the parent compound, that is, their stability towards photocatalysis is good. Most importantly, **1** shows a remarkable photodegra-

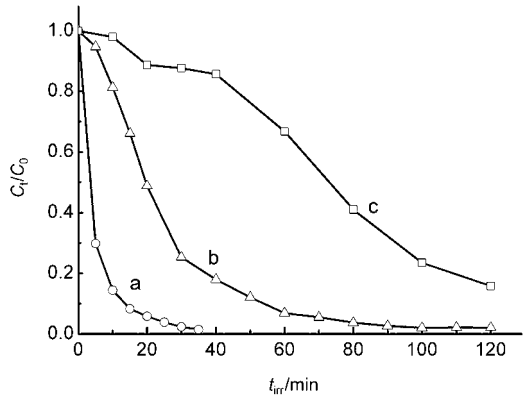

Figure 5. Concentration changes of RhB irradiated with UV light as a function of irradiation time t_{irr} in the presence of a) **1**, b) **2**, and c) Degussa P-25. C_t and C_0 stand for the RhB concentrations after and before irradiation.

dation activity for RhB when a xenon lamp is used as the irradiation source for simulation of sun light (Figure 6). The main part of the radiation from the xenon lamp is in the wavelength region longer than 400 nm. Illumination of RhB with xenon light in the absence of particulate **1** leads to no degradation of the dye at all, that is, RhB degradation needs an electron-transfer mediator under visible light. For comparison, the visible-light photocatalytic performance of P-25 was also tested, and it showed only slight photocatalytic activity under xenon-light irradiation. Compound **2** does not show photocatalytic activity when irradiated for 240 min with the xenon lamp, since this compound can hardly be excited by visible light, as suggested by its UV/Vis absorption properties. Structural difference between **1** and **2** lead to the discrepancy in photocatalytic activity, and the relationship between the structures and the physical properties is further elucidated below. The UV/Vis absorptions of **1** and **2** are also related to their structures, and in this sense any photocatalytic discrepancy between **1** and **2** resulting from the UV/Vis absorption properties may trace back to the structural differences of these two materials.

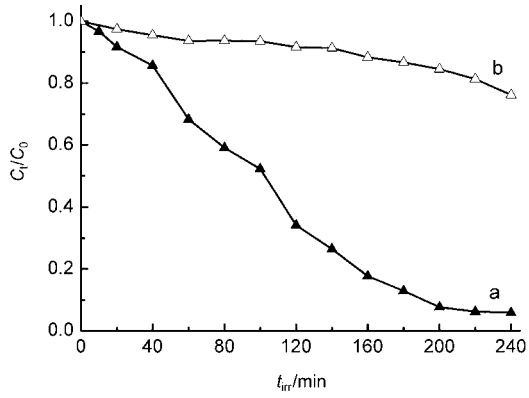

Figure 6. Concentration changes of RhB under irradiation with xenon-lamp light in the presence of a) **1** and b) Degussa P-25.

The decrease in total organic carbon (TOC) reaches about 34 and 40% when the solution color completely disappears under UV irradiation for **1** and **2**, respectively, and about 30% after 240 min of Xe-lamp irradiation in the presence of **1**. The TOC analysis confirmed mineralization of RhB to a considerable extent in the presence of **1** or **2**. Ion chromatography analysis indicated that NO_3^- ions are the N-containing species with the highest stable oxidation state of nitrogen formed in the degraded solution. The percentages of RhB converted into NO_3^- ions were about 30 and 34% after 40 min of UV and Xe-light irradiation, respectively, in the presence of **1**, and about 25% after 120 min of UV irradiation in the presence of **2**. The substoichiometric amount of NO_3^- ions may be partly due to strong sorption of NO_3^- ions on the surface of the photocatalysts.[34] Irradiation for longer times of the decolorized solutions leads to no change in NO_3^- concentration for these systems, except for the case in which UV light is used in the presence of **1** and the NO_3^- concentration clearly decreases, probably due to decomposition. In addition, the formation of formic and acetic acids in the final products of the photocatalytic systems was also observed by ion chromatography.

Typical intermediate species generated in the degradation of RhB photocatalyzed by **1** or **2** were identified from positive-ion ($M+H$) mass spectra. In each case, the dye was mostly degraded from *m/z* 443.2 (RhB) to *m/z* 415.2 (*N*,*N*′,*N*′-triethylrhodamine), 387.1 (*N*,*N*′-diethylrhodamine), 359.0 (*N*-ethylrhodamine), corresponding to stepwise loss of C_2H_5 units.[33,34] Decarboxylated species were also observed, corresponding to a mass spectral signal at *m/z* 260.2.[34] At the end of the photocatalytic reaction, a marked decrease is noted in signal intensity at *m/z* 443.2, which indicates that RhB has effectively been photodegraded into final products with lower molecular weight, such as formic and acetic acids, as confirmed by ion chromatography.

Photocatalytic reaction mechanism: The photochemistry of uranyl compounds dates back to the early 1800s. Since then, their photochemistry, especially photocatalytic performance, has been studied extensively.[35] Generally, two mechanisms have been proposed for the photocatalytic reactions involving U^{VI} species, that is, hydrogen abstraction and electron transfer.[35] The detection of radicals, mostly as a result of the loss of α-H, from various organic compounds including carboxylic acids, ketones, aldehydes, alcohols, esters, and amides supported the hydrogen-abstraction mechanism,[21a,36] whereas the relationships between quenching rate and ionization potential (IP) suggest an electron-transfer pathway for reactions involving aromatic hydrocarbons.[37] Recently, quenching experiments on alkenes and dienes also supported the electron-transfer pathway.[38] It seems that the α-H atoms of molecules with electron-withdrawing groups are likely to be abstracted, while substrates with electron-rich π or conjugated π systems readily undergo electron-transfer reactions. As evidenced by our UV/Vis and mass spectral studies, the RhB molecules with electron-drawing N atom (see Scheme 1 for the structure of RhB) lose ethyl groups

stepwise, that is, the hydrogen-abstraction mechanism is favorable, because the electron-transfer pathway most likely leads to decomposition of the conjugated system rather than deethylation.

Despite the differences between the decomposition pathways discussed above, both mechanisms involve photoexcitation of the uranyl species. U^{VI} is not a strongly oxidizing species (UO_2^{2+}/UO_2^{+} 0.06 V).[39] However, on excitation of this species, the resulting $*UO_2^{2+}$ is very active and can trigger a variety of redox reactions due to its high oxidation potential of approximately 2.6 V.[38,40] As reported and quite clearly elucidated in the literature, excited uranyl ions in aqueous solution can lead to the oxidation of organic molecules in the presence of oxygen or H_2O_2.[21,41] Nevertheless, no solid U^{VI} compounds have been reported to show photocatalytic properties prior to our work. Recently, we reported that uranyl groups incorporated into a coordination polymer exibit photocatalytic activity.[23] Although the photocatalytic tests on **1** and **2** were carried out in heterogeneous systems, it is believed that the uranyl center photocatalytically behaves in a way similar to that in solution. The uranyl center in the two compounds can be excited by photons with enough energy, and one electron in the HOMO jumps to the LUMO. Because the energies of the 5f, 6d, 7p, and 7s orbitals of uranium are comparable, it is quite difficult, and sometimes even impossible, to determine the electron configuration and orbital combination in uranium compounds.[42] However, the detailed electronic structures of the compounds are not necessary for elucidating the photocatalytic reaction mechanism, and a simplified model is sufficient for our discussion (Scheme 1). Despite the disputable electron configuration and orbital combination, it is still clear that the double bonds between uranium and oxygen are involved in photoexcitation.[43] Because the HOMO is mainly contributed to by oxygen 2p bonding orbitals and the LUMO by empty uranium orbitals,[44] charge transfer actually takes place from oxygen to uranium on photoexcitation to give uranium in the +5 and oxygen in the −1 oxidation state. The electron of the excited state in the LUMO is usually very easily lost, while the HOMO strongly demands one electron to return to its stable state. Generally, the excited $*UO_2^{2+}$ decays to its ground state quickly. However, if some molecules are within a reasonable range and have an appropriate orientation, for example, RhB in this case, transitional active complexes can be formed. Thus, one α-hydrogen atom of the methylene group bonded to the electron-withdrawing nitrogen atom of RhB, which will give up its electron and leave as H^+ later,[35,45] is abstracted by uranyl species, and this results in the cleavage of the C–N bond and stepwise *N*-deethylation of RhB (Scheme 2). Since the HOMO is then reoccupied, the excited electron must remain in the LUMO until it is captured by electronegative substances such as molecular oxygen in solution, which would transform into highly active peroxide anion and subsequently accomplish further oxidation and total degradation of RhB.[46]

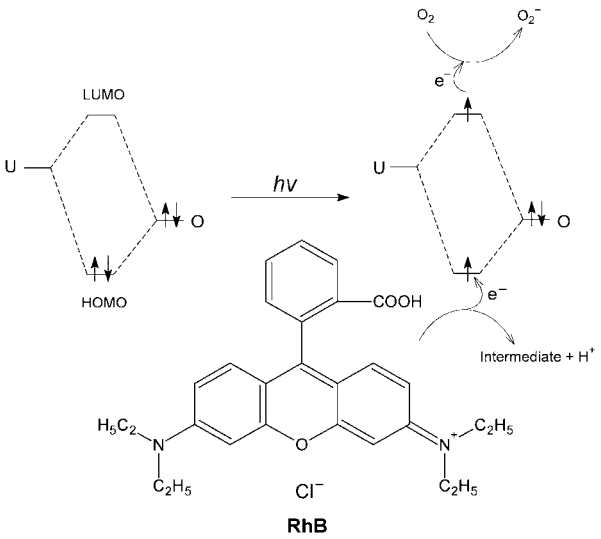

Scheme 1. Photoexcitation of **1** or **2** and oxidation of the RhB substrate.

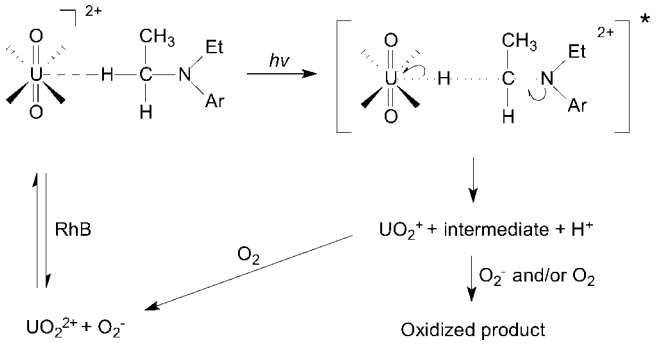

Scheme 2. Proposed photodegradation pathways of the RhB substrate in the presence of **1** or **2**.

We examined the function of oxygen in the photocatalysis mechanism by monitoring the photocatalytic activities in the presence or absence of oxygen in the photodegradation systems. When argon is bubbled through the system for 30 min before and during irradiation, the photocatalytic reaction rate decreases rapidly for **1** and drops to zero for **2**. In the light of these results, the presence of oxygen is essential for the photocatalytic reaction to proceed, because otherwise the uranium(v) species cannot be oxidized back to U^{VI} for a new cycle.[46] The peroxide anion formed from the molecular oxygen is an important intermediate for the further degradation of RhB. Note that the photocatalytic reactor we used was not sealed, and the oxygen in the reaction system could hardly be removed completely. Compound **1** is so active that traces of oxygen present in the reaction system degrade RhB effectively when **1** is used as photocatalyst.

Spin-trap ESR was used for the detection of possibly formed hydroxyl radicals. However, it gave no characteristic signals, that is, no hydroxyl radicals were involved in our reactions. Neither could peroxide anion be detected, probably due to its high instability in aqueous solution, as few exam-

ples of its detection in aqueous solution have been reported in photocatalytic systems so far.[32] Hydroxyl radicals may be involved in a variety of photocatalytic reactions, but they are not necessary in some reported cases.[32,47] Moreover, although the spin signals were recorded in the case of TiO_2, it is still argued that the signals do not really arise from hydroxyl radicals,[47] and in fact the hydroxyl radicals are not important or even are not formed at all.[48] When active centers react with substrates directly, as proposed in our case, hydroxyl radicals could also be absent.

Sometimes the excitation of the catalyst is not needed in photocatalytic reactions. For example, although TiO_2 has no significant light absorption in the visible region, the excitation of dye molecules and electron injection into TiO_2 still make it possible to decompose the dye molecules on the surface of TiO_2.[49] However, noting the difference in photocatalytic activity between **1** and **2** under irradiation with visible light, we consider that in the photocatalytic reaction, the excitation of our catalysts is much more important than that of the dye molecules themselves. Although RhB is undoubtedly excited in this case (under visible-light irradiation), **1** can form the charge-transfer excitation state in the visible region, as confirmed by the solid-state UV/Vis spectrum, and shows pronounced activity, while **2** is almost inactive under the same conditions because its double-bond $O_{2p}\rightarrow U$ charge-transfer electron transition is beyond the energy of visible light. The conclusion that excitation of the catalyst is more important than that of dye molecules is also in harmony with the fact that **1** is distinctly more efficient than P-25 under visible light.

The difference in catalytic activity under UV irradiation between **1** and **2** arises from the discrepancy in crystal structure of the two compounds. First, the uranium atom is seven-coordinate in **1**, while in **2** it is eight-coordinate. The fewer ligands around the uranium center in **1** mean that steric hindrance preventing access of the dye substrate to the U center of the catalyst is reduced, and the U center is more free to form catalyst–substrate complex transition states. On the other hand, the silver-centered species in **1** are packed almost parallel to the uranyl–organic layers, while in **2** they rather occupy the interlayer space because their orientation is vertical to the uranyl–organic layers. The more spacious interlayer region of **1** makes it easier for the branch of the substrate dye molecule to penetrate and to gain access to the active excited U centers of the interlayer region (near the layer edges) in **1**, whereas **2** has a less spacious interlayer region and fully coordinated U centers, which are unfavorable for the access of the dye molecules. Based on the comparisons above, it is easy to understand the different photocatalytic activities of the two compounds under UV irradiation. For irradiation under visible light, the activity difference mainly arises from the difference in visible-light excitation between **1** and **2**, as observed in the UV/Vis absorption spectra. The dependence of photocatalytic activity on structural features has been demonstrated for other uranyl-containing compounds as well. For instance, the microporous $[Ni_2(H_2O)_2(qa)_2(bipy)_2U_5O_{14}(H_2O)_2(OAc)_2]\cdot 2H_2O$ (HOAc = acetic acid, bipy = 4,4′-bipyridine, H_2qa = quinolinic acid), in which all five uranyl centers are closely bridged to ribbons so that only the ribbon edges can be attacked by the substrate molecules, shows relative low photocatalytic activity for RhB degradation, although it is active for the degradation of the easily degradable methyl blue,[23] whereas $[(ZnO)_2(UO_2)_3(na)_4(OAc)_2]$ (Hna = nicotinic acid), built up from inorganic U-O-Zn-clustered double sheets,[22] and the well-known thermal catalysts UO_3 and U_3O_8, in which all U−O species are crystallized together,[50] are inactive under identical conditions, since they can hardly form transition complexes with RhB due to the poor accessibility of their U centers to RhB molecules. Therefore, our compounds, especially **1**, are a unique type of coordination polymers with uranyl units that exhibit high photocatalytic activity for dye degradation because of the accessibility of their U centers, which can be photoexcited by UV or visible light.

Conclusion

By hydrothermal reaction routes, two novel 2D silver–uranium–organic assembly compounds **1** and **2** were crystallized, and it was demonstrated that these two water-insoluble solids have distinct photocatalytic properties. Both structures are composed of uranyl species, Ag–organic components, and bridging ligands. In the structure of **1**, the uranyl units are connected by bridging bdc ligands to produce chains, which are then cross-linked by additional bdc groups to form a 2D network decorated with $[Ag(bipy)]^+$ subunits. The structure of **2** consists of 2D layers with Ag-UO_8-Ag trinuclear cores as building blocks, which are linked by bridging btec ligands. These two uranyl-containing compounds are photostable, and they exhibit photocatalytic activities higher than that of commercial TiO_2 (Degussa P-25) under UV irradiation for the oxidation and mineralization of rhodamine B as a model pollutant which is recognized as being difficult to degrade. Most strikingly, **1** also shows photocatalytic activity under visible-light irradiation. Furthermore, **1** is photocatalytically more active than **2** because of structural differences. The presence of uranyl species, which can be photoexcited and effectively activate the dye molecules, is responsible for the photocatalytic performance of the two compounds. The successful synthesis of **1** and **2** provides access to a promising path in the search for stable new photodegradation catalysts.

Experimental Section

Materials and methods: Chemicals for synthesis were commercially available and used as received without further purification. The uranium oxides UO_3 and U_3O_8 were prepared by following procedures described in the literature.[51] Elemental microanalyses (C, H, N) were conducted on a Perkin-Elmer 2400 elemental analyzer, and metal contents were determined by inductively coupled plasma (ICP) analysis on a Perkin-Elmer Optima 3300DV ICP spectrometer.

The powder XRD patterns ($Cu_{K\alpha}$ radiation, $\lambda = 1.5418$ Å) were recorded on a Siemens D5005 diffractometer with a graphite monochromator at room temperature. The FTIR spectra of the samples dispersed in KBr pellets were obtained in the range 4000–400 cm^{-1} on a Nicolet Impact 410 FTIR spectrometer. TG/DTA was conducted on a Netzsch STA 449C thermal analyzer under a flow of dry air at a heating rate of 20 $K\,min^{-1}$. The solid-state diffuse-reflectance UV/Vis spectra for powder samples were recorded on a Perkin-Elmer Lambda 20 UV/Vis spectrometer equipped with an integrating sphere by using $BaSO_4$ as a white standard, and the reflection intensity data were converted to Kubelka–Munk units.

$[Ag(bipy)(UO_2)(bdc)_{1.5}]$ (1): In a typical preparation, an aqueous mixture (10 mL) containing $UO_2(OAc)_2{\cdot}2H_2O$ (0.21 g, 0.0005 mol), $AgNO_3$ (0.17 g, 0.001 mol), bipy (0.16 g, 0.001 mol), H_2bdc (0.16 g, 0.001 mol), and water (10.00 g, 0.556 mol) in a molar ratio of 1:2:2:2:1110 was sealed in a Teflon-lined autoclave (15 mL) and heated at 160 °C for 3 d. After filtration, washing thoroughly with distilled water in an ultrasonic bath for a few minutes to remove amorphous impurities, and air-drying at ambient temperature, yellow block crystals were obtained in about 50% yield (0.35 g) on the basis of U. The product was stable in air and insoluble in water and common organic solvents such as ethanol, acetone, and acetonitrile. Moreover, no changes in color or powder XRD pattern of the compound could be detected after direct irradiation with a 400 W UV lamp for about 90 min. Thus, **1** is insensitive to photodecomposition, whereas many silver(I) compounds are unstable under UV irradiation.[52] Elemental analysis calcd (%) for $C_{22}H_{14}AgN_2O_8U$: C 33.84, H 1.79, N 3.59, Ag 13.84; found: C 33.68, H 1.71, N 3.51, Ag 13.80; Main IR features (KBr): $\tilde{\nu} = 1590$s, 1555m, 1520s, 1438m, 1391s, 1345s, 1147w, 1104w, 1019w, 920s, 850w, 830w, 750s, 530m, 503w, 469 cm^{-1} w.

$[Ag_2(phen)_2UO_2(btec)]$ (2): The synthetic procedure for **2** was identical to that for **1**, except that instead of bipy and $bdcH_2$, phen (0.20 g, 0.001 mol) and H_4btec (0.25 g, 0.001 mol) were used as ligands. Yellow block crystals were obtained in about 73% yield (0.40 g). This compound was also insoluble in water and common organic solvents and photostable under UV irradiation. Elemental analysis calcd (%) for $C_{34}H_{18}Ag_2N_4O_{10}U$: C 37.22, H 1.64, N 5.11, Ag 19.70; found: C 38.01, H 1.70, N 5.22, Ag 19.80; Main IR features (KBr): $\tilde{\nu} = 1617$m, 1553s, 1482w, 1429s, 1353s, 1306s, 1122m, 913m, 848s, 807w, 767w, 723 m, 671w, 629w, 569w, 521 cm^{-1} m.

X-ray crystal structure determination: Yellow blocks of **1** with approximate crystal size of $0.36 \times 0.28 \times 0.20$ mm and **2** of $0.23 \times 0.22 \times 0.17$ mm were selected, and the single-crystal X-ray data were recorded at 293(2) K on a Bruker Smart-CCD diffractometer ($Mo_{K\alpha}$, $\lambda = 0.71073$ Å). The structures were solved by direct methods (SHELXTL Version 5.10), and refined by full-matrix least-squares techniques on F^2. All non-hydrogen atoms were refined anisotropically and the aromatic hydrogen atoms were calculated and fixed with thermal parameters based on the bonded carbon atoms (C–H 0.93 Å). A total of 3738 reflections out of 6014 unique reflections were independent in the range $2.45 < \theta < 25.07°$ and were used to solve the structure for **1** ($R_{int} = 0.0512$) [$I > 2\sigma(I)$]. Of the total of 11388 unique reflections for **2** collected in the range of $1.88 < \theta < 30.03°$, 4265 reflections were unique ($R_{int} = 0.0472$) [$I > 2\sigma(I)$].

CCDC 224855 (**1**) and CCDC-224856 (**2**) contain the supplementary crystallographic data for this paper. These data can be obtained free of charge from The Cambridge Crystallographic Data Centre via www.ccdc.cam.ac.uk/data_request/cif.

Photocatalytic testing: Photocatalytic experiments in aqueous solution were performed in a water-cooled quartz (for Hg lamp, UV light) or Pyrex (for Xe lamp) cylindrical cell. The reaction mixture in the cell was maintained at 20±2 °C by a continuous flow of water through an external cooling coil with magnetic stirring, and were illuminated from an internal light source with about 2-cm optical path length. The UV light source was a 125 W high-pressure mercury lamp (HPML, main output 313.2 nm). To address the activity in the visible range, solar-light experiments were performed with a 400 W Xe lamp (radiation wavelength >400 nm).

The photocatalytic activities of the two compounds were compared with that of commercial TiO_2 (Degussa P-25), which is a well-known photocatalyst working under UV irradiation. A suspension of powdered catalyst (160 mg) in a fresh aqueous solution of RhB (80 mL, 0.10 $mmol\,L^{-1}$) was ultrasonicated for 5 min and magnetically stirred in the dark for at least 30 min (to establish an adsorption/desorption equilibrium of RhB on the sample surface) until no change in the UV/Vis absorption of the RhB solution occurred. At given irradiation time intervals, a series of aqueous solutions of a certain volume were collected and filtered through a Millipore filter to remove suspended catalyst particles for analysis. The photocatalytic performance of the catalysts was estimated by monitoring the visible absorbance (at $\lambda = 555$ nm) characteristic of the target (RhB) by UV/Vis spectroscopy. The mineralization of the dye in the degraded solutions was assessed by measuring the TOC on a Shimadzu TOC-V_{CPH} analyzer. Since the molar absorptivity of the dye was very high, the sample after filtration was diluted by a factor of 2 to accurately quantify the dye concentration. The final products after photocatalytic degradation process were analyzed by a DX-300 ion chromatograph (Dionex) equipped with a conductivity detector. An AS4A anion column and an ICE-ASI anion column were used for determination of NO_3^- ions quantitatively and organic acids qualitatively, respectively. Other highly polar and less volatile intermediate products in aqueous solution during the photocatalytic process were investigated with an Agilent 1100 LC-MS VL system. Spin-trap technique with 5,5-dimethyl-1-pyrroline-*N*-oxide (DMPO) was performed on a Bruker EPR 300E spectrometer to detect hydroxyl radicals in the suspension containing powdered catalyst after irradiation under UV light for 120 s at room temperature.

Acknowledgements

This work was financially supported by the National Natural Science Foundation of China and the Education Ministry of China. The authors thank Prof. Y. H. Guo of Northeast Normal University and Prof. J. C. Zhao of Institute of Chemistry, the Chinese Academy of Sciences for their kind help.

[1] a) P. H. Dinolfo, J. T. Hupp, *Chem. Mater.* **2001**, *13*, 3113–3125; b) S. R. Batten, R. Robson, *Angew. Chem.* **1998**, *110*, 1558–1595; *Angew. Chem. Int. Ed.* **1998**, *37*, 1460–1494; c) P. J. Hagrman, D. Hagrman, J. Zubieta, *Angew. Chem.* **1999**, *111*, 2798–2848; *Angew. Chem. Int. Ed.* **1999**, *38*, 2638–2684; d) G. Férey, *Chem. Mater.* **2001**, *13*, 3084–3098; e) L. Pan, H. Liu, X. Lei, X. Huang, D. H. Olson, N. J. Turro, J. Li, *Angew. Chem.* **2003**, *115*, 560–564; *Angew. Chem. Int. Ed.* **2003**, *42*, 542–546; f) A. N. Khlobystov, A. J. Blake, N. R. Champness, D. A. Lemenovskii, A. G. Majouga, N. V. Zyk, M. Schröder, *Coord. Chem. Rev.* **2001**, *222*, 155–192.

[2] a) M. Eddaoudi, D. B. Moler, H. Li, B. Chen, T. M. Reineke, M. O'Keeffe, O. M. Yaghi, *Acc. Chem. Res.* **2001**, *34*, 319–330; b) N. Snejko, E. Gutiérrez-Puebla, J. L. Martínez, M. A. Monge, C. Ruiz-Valero, *Chem. Mater.* **2002**, *14*, 1879–1883; c) S. S.-Y. Chui, S. M.-F. Lo, J. P. H. Charmant, A. G. Orpen, I. D. Williams, *Science* **1999**, *283*, 1148–1150.

[3] a) F. Serpaggi, G. Férey, *J. Mater. Chem.* **1998**, *8*, 2737–2741; b) T. M. Reineke, M. Eddaoudi, M. Fehr, D. Kelley, O. M. Yaghi, *J. Am. Chem. Soc.* **1999**, *121*, 1651–1657; c) C. Piguet, C. Edder, S. Rigault, G. Bernardinelli, J.-C. G. Bünzli, G. Hopfgartner, *J. Chem. Soc. Dalton Trans.* **2000**, 3999–4006; d) Z. Zheng, *Chem. Commun.* **2001**, 2521–2529; e) F. A. A. Paz, J. Klinowski, *Chem. Commun.* **2003**, 1484–1485.

[4] a) J.-Y. Kim, A. J. Norquist, D. O'Hare, *Chem. Mater.* **2003**, *15*, 1970–1975; b) J.-Y. Kim, A. J. Norquist, D. O'Hare, *Dalton Trans.* **2003**, 2813–2814; c) L. A. Borkowski, C. L. Cahill, *Inorg. Chem.* **2003**, *42*, 7041–7045.

[5] a) L. Salmon, P. Thuéry, E. Rivière, J.-J. Girerd, M. Ephritikhine, *Dalton Trans.* **2003**, 2872–2880; b) T. L. Borgne, E. Rivière, J. Marrot, P. Thuéry, J.-J. Girerd, M. Ephritikhine, *Chem. Eur. J.* **2002**, *8*, 774–783; c) R. J. Francis, P. S. Halasyamani, D. O'Hare, *Angew. Chem.* **1998**, *110*, 2336–2339; *Angew. Chem. Int. Ed.* **1998**, *37*, 2214–2217; d) P. B. Duval, C. J. Burns, D. L. Clark, D. E. Morris, B. L.

Scott, J. D. Thompson, E. L. Werkema, L. Jia, R. A. Andersen, *Angew. Chem.* **2001**, *113*, 3461–3465; *Angew. Chem. Int. Ed.* **2001**, *40*, 3357–3361.
[6] a) A. C. Bean, S. M. Peper, T. E. Albrecht-Schmitt, *Chem. Mater.* **2001**, *13*, 1266–1272; b) Z. T. Yu, G. H. Li, Y. S. Jiang, J. J. Xu, J. S. Chen, *Dalton Trans.* **2003**, 4219–4220.
[7] a) G. J. Hutchings, C. S. Heneghan, I. D. Hudson, S. H. Taylor, *Nature* **1996**, *384*, 341–343; b) S. H. Taylor, C. S. Heneghan, G. J. Hutchings, I. D. Hudson, *Catal. Today* **2000**, *59*, 249–259.
[8] a) R. G. Peters, B. P. Warner, C. J. Burns, *J. Am. Chem. Soc.* **1999**, *121*, 5585–5586; b) Y. Li, C. L. Cahill, P. C. Burns, *Chem. Mater.* **2001**, *13*, 4026–4031.
[9] a) F. G. N. Cloke, P. B. Hitchoock, *J. Am. Chem. Soc.* **2002**, *124*, 9352–9353; b) W. J. Evans, S. A. Kozimor, J. W. Ziller, *J. Am. Chem. Soc.* **2003**, *125*, 14264–14265.
[10] a) M. R. Hoffmann, S. T. Martin, W. Choi, D. W. Bahnemann, *Chem. Rev.* **1995**, *95*, 69–96; b) D. S. Bhatkhande, V. G. Pangarkar, A. A. Beenackers, *J. Chem. Technol. Biotechnol.* **2001**, *77*, 102–116; c) K. Rajeshwar, N. R. de Tacconi, C. R. Chenthamarakshan, *Chem. Mater.* **2001**, *13*, 2765–2782; d) B. Meunier, *Science* **2002**, *296*, 270–271.
[11] a) A. Fujishima, K. Honda, *Nature* **1972**, *238*, 37–38; b) M. Hara, J. T. Lean, T. E. Mallouk, *Chem. Mater.* **2001**, *13*, 4668–4675; c) O. Khaselev, J. A. Turner, *Science* **1998**, *280*, 425–427; d) M. Hara, T. E. Mallouk, *Chem. Commun.* **2000**, 1903–1904; e) Z. Zou, J. Ye, K. Sayama, H. Arakawa, *Nature* **2001**, *414*, 625–627.
[12] a) E. Papaconstantinou, *Chem. Soc. Rev.* **1989**, *18*, 1–31; b) J. Yoshimura, Y. Ebina, J. Kondo, K. Domen, A. Tanaka, *J. Phys. Chem.* **1993**, *97*, 1970–1973; c) G. B. Saupe, T. E. Mallouk, W. Kim, R. H. Schmehl, *J. Phys. Chem. B* **1997**, *101*, 2508–2513.
[13] S. Sakthivel, H. Kisch, *Angew. Chem.* **2003**, *115*, 5057–5060; *Angew. Chem. Int. Ed.* **2003**, *42*, 4908–4911.
[14] a) S. G. Yan, L. A. Lyon, B. L. Lemon, J. S. Preiskorn, J. T. Hupp, *J. Chem. Educ.* **1997**, *74*, 657–662; b) K. G. Kim, D. W. Hwang, J. S. Lee, *J. Am. Chem. Soc.* **2004**, *126*, 8912–8913; c) Z. Lei, W. You, M. Liu, G. Zhou, T. Takata, M. Hara, K. Domen, C. Li, *Chem. Commun.* **2003**, 2142–2143.
[15] R. Asahi, T. Morikawa, T. Ohwaki, K. A. Y. Taga, *Science* **2001**, *293*, 269–271.
[16] A. Ishikawa, T. Takata, J. Kondo, M. Hara, H. Kobayashi, K. Domen, *J. Am. Chem. Soc.* **2002**, *124*, 13547–13553.
[17] S. U. M. Khan, M. Al-Shahry, W. B. Ingler Jr., *Science* **2002**, *297*, 2243–2245.
[18] I. Justicia, P. Ordejón, G. Canto, J. L. Mozos, J. Fraxedas, G. A. Battiston, R. Gerbasi, A. Figueras, *Adv. Mater.* **2002**, *14*, 1399–1402.
[19] a) A. Kudo, K. Omori, H. Kato, *J. Am. Chem. Soc.* **1999**, *121*, 11459–11467; b) D. G. Shchukin, R. A. Caruso, *Adv. Funct. Mater.* **2003**, *13*, 789–794; c) H. Weiß, A. Fernandez, H. Kisch, *Angew. Chem.* **2001**, *113*, 3942–3945; *Angew. Chem. Int. Ed.* **2001**, *40*, 3825–3827; d) A. Di Paola, L. Palmisano, A. M. Venezia, V. Augugliaro, *J. Phys. Chem. B* **1999**, *103*, 8236–8244.
[20] a) S. G. Yan, J. T. Hupp, *J. Phys. Chem.* **1996**, *100*, 6867–6870; b) G. Sivalingam, K. Nagaveni, M. S. Hegde, G. Madras, *Appl. Catal. B* **2003**, *45*, 23–38.
[21] a) A. Bakac, J. H. Espenson, *Inorg. Chem.* **1995**, *34*, 1730–1735; b) S. M. Fonseca, H. D. Burrows, M. G. Miguel, M. Sarakha, M. Bolte, *Photochem. Photobiol. Sci.* **2004**, *3*, 317–321; c) T. M. Mccleskey, T. M. Foreman, E. E. Hallman, C. J. Burns, N. N. Sauer, *Environ. Sci. Technol.* **2001**, *35*, 547–551.
[22] W. Chen, H. M. Yuan, J. Y. Wang, Z. Y. Liu, J. J. Xu, M. Yang, J. S. Chen, *J. Am. Chem. Soc.* **2003**, *125*, 9266–9267.
[23] Z. T. Yu, Z. L. Liao, Y. S. Jiang, G. H. Li, G. D. Li, J. S. Chen, *Chem. Commun.* **2004**, 1814–1815.
[24] C. Zhang, C. Janiak, *J. Chem. Crystallogr.* **2001**, *31*, 29–35.
[25] a) R. C. Finn, J. Zubieta, *J. Chem. Soc. Dalton Trans.* **2002**, 856–861; b) X. M. Chen, G. F. Liu, *Chem. Eur. J.* **2002**, *8*, 4811–4817.
[26] M. B. Doran, A. J. Norquist, D. O'Hare, *Chem. Mater.* **2003**, *15*, 1449–1455.
[27] A. C. Bean, C. F. Campana, O. Kwon, T. E. Albrecht-Schmitt, *J. Am. Chem. Soc.* **2001**, *123*, 8806–8810.
[28] S. L. Zheng, J. P. Zhang, W. T. Wong, X. M. Chen, *J. Am. Chem. Soc.* **2003**, *125*, 6882–6883.
[29] C. Janiak, *J. Chem. Soc. Dalton Trans.* **2000**, 3885–3896.
[30] a) V. A. Volkovich, T. R. Griffiths, D. J. Fray, R. C. Thied, *Phys. Chem. Chem. Phys.* **2001**, *3*, 5182–5191; b) P. M. Almond, T. E. Albrecht-Schmitt, *Inorg. Chem.* **2002**, *41*, 1177–1183.
[31] a) R. S. Addleman, M. Carrott, C. M. Wai, T. E. Carleson, B. W. Wenclawiak, *Anal. Chem.* **2001**, *73*, 1112–1119; b) J. Huang, X. Wang, A. J. Jacobson, *J. Mater. Chem.* **2003**, *13*, 191–196; c) H. Kunkely, A. Vogler, *Z. Naturforsch. B* **2002**, *57*, 301–304.
[32] W. Ma, J. Li, X. Tao, J. He, Y. Xu, J. C. Yu, J. Zhao, *Angew. Chem.* **2003**, *115*, 1059–1062; *Angew. Chem. Int. Ed.* **2003**, *42*, 1029–1032.
[33] S. Horikoshi, A. Saitou, H. Hidaka, N. Serpone, *Environ. Sci. Technol.* **2003**, *37*, 5813–5822.
[34] Y. Guo, C. Hu, C. Jiang, Y. Yang, S. Jiang, X. Li, E. Wang, *J. Catal.* **2003**, *217*, 141–151.
[35] H. D. Burrows, T. J. Kemp, *Chem. Soc. Rev.* **1974**, *3*, 139–165.
[36] a) D. Greatorex, R. J. Hill, T. J. Kemp, T. J. Stone, *J. Chem. Soc. Faraday Trans. 1* **1972**, *68*, 2059–2076; b) W. D. Wang, A. Bakac, J. H. Espenson, *Inorg. Chem.* **1995**, *34*, 6034–6039.
[37] a) R. Matsushima, S. Sakuraba, *J. Am. Chem. Soc.* **1971**, *93*, 7143–7145; b) R. Matsushima, *J. Am. Chem. Soc.* **1972**, *94*, 6010–6016.
[38] T. M. McCleskey, C. J. Burns, W. Tumas, *Inorg. Chem.* **1999**, *38*, 5924–5925.
[39] F. A. Cotton, G. Wilkinson, *Advanced Inorganic Chemistry*, 5th ed., Wiley, New York, **1988**, Chap. 21, pp. 989–990.
[40] M. Sarakha, M. Bolte, H. D. Burrows, *J. Photochem. Photobiol. A* **1997**, *107*, 101–106.
[41] D. H. Volman, J. R. Seed, *J. Am. Chem. Soc.* **1964**, *86*, 5095–5098.
[42] F. A. Cotton, G. Wilkinson, *Advanced Inorganic Chemistry*, 5th ed., Wiley, New York, **1988**, Chap. 21, pp. 980–984.
[43] C. K. Jørgensen, *J. Lumin.* **1979**, *10*, 63–68.
[44] a) M. J. Sarsfield, H. Steele, M. Helliwell, S. J. Teat, *Dalton Trans.* **2003**, 3443–3449; b) R. G. Denning, *Struct. Bonding (Berlin)* **1992**, *79*, 215–276; c) V. C. Williams, M. Müller, M. A. Leech, R. G. Denning, M. L. H. Green, *Inorg. Chem.* **2000**, *39*, 2538–2541.
[45] a) W. D. Jones, *Science* **2000**, *287*, 1942–1943; b) W. D. Jones, *Acc. Chem. Res.* **2003**, *36*, 140–146.
[46] a) Y. Mao, A. Bakac, *Inorg. Chem.* **1996**, *35*, 3925–3930; b) D. A. Nivens, Y. Zhang, S. M. Angel, *J. Photochem. Photobiol. A* **2002**, *152*, 167–173.
[47] R. Nakamura, Y. Nakato, *J. Am. Chem. Soc.* **2004**, *126*, 1290–1298.
[48] K. Ishibashi, A. Fujishima, T. Watanabe, K. Hashimoto, *J. Photochem. Photobiol. A* **2000**, *134*, 139–142.
[49] a) K. A. Walters, D. A. Gaal, J. T. Hupp, *J. Phys. Chem. B* **2002**, *106*, 5139–5142; b) K. E. Splan, A. M. Massari, J. T. Hupp, *J. Phys. Chem. B* **2004**, *108*, 4111–4115; c) T. X. Wu, G. M. Liu, J. C. Zhao, H. Hidaka, N. Serpone, *J. Phys. Chem. B* **1998**, *102*, 5845–5851.
[50] a) P. C. Debets, *Acta Cardiol.* **1966**, *21*, 589–593; b) R. Herak, *Acta Crystallogr. Sect. B* **1969**, *25*, 2505–2508.
[51] F. A. Cotton, G. Wilkinson, *Advanced Inorganic Chemistry*, 5th ed., Wiley, New York, **1988**, Chap. 21, pp. 1003–1010.
[52] a) F. Sabin, C. K. Ryu, P. C. Ford, A. Vogler, *Inorg. Chem.* **1992**, *31*, 1941–1945; b) H. L. Zhu, X. M. Zhang, G. F. Liu, D. Q. Wang, *Z. Anorg. Allg. Chem.* **2003**, *629*, 1059–1062.

Received: November 22, 2004
Published online: February 24, 2005